Formation of Metallosupramolecular Polymers within Highly Ordered Silica Mesochannels

Mutsumi Kimura,* Yayoi Iwashima, Kazuchika Ohta, Kenji Hanabusa, and Hirofusa Shirai*

PRESTO (Organization and Function), Japan Science and Technology Agency (JST), Department of Functional Polymer Science, Faculty of Textile Science and Technology, Shinshu University, Ueda 386-8567, Japan

Received November 12, 2004; Revised Manuscript Received April 9, 2005

ABSTRACT: Amphiphilic block copolymer $EO_{20}PO_{70}EO_{20}$ (M_n = 5800 g/mol) has been modified with terpyridine (tpy) end groups as a building block for the construction of metallosupramolecular polymers. The synthesized tpy-terminated $EO_{20}PO_{70}EO_{20}$ **1** assembles into a linear supramolecular polymer by a metal−ligand interaction between two tpy terminates of **1** and one iron ion. Use of $EO_{20}PO_{70}EO_{20}$ having tpy terminates **1** as a template for the sol−gel polymerization of tetraethoxysilane (TEOS) results in the preparation of well-ordered hexagonal mesoporous silica structure, in which **1** is filled within highly ordered mesoporous silica channels. The incorporated tpy-terminated copolymers assemble into metallosupramolecular polymers by the formation of metal complexes within the silica mesochannels.

Introduction

Synthesis of mesoporous materials under the templates of supramolecular molecular assemblies is an area of rapid growth with various applications in many fields such as catalysis, membrane and separation technology, and molecular engineering.[1] Mesoporous materials provide a well-ordered alignment of nanometer-sized channels with an internal space. Recent interest in incorporating functional organic materials within inorganic channels has highlighted applications in shape-selective catalysts and directional electron/energy transfer devices.[1a,1d,1e]

One approach to preparing these organic−inorganic composites is to incorporate functional guest molecules within preformed mesoporous materials.[2] This approach on the basis of host−guest chemistry, however, results in an uneven infiltration of the guest functional molecules into the channels. In contrast, several organic−inorganic composites have been prepared by polymerizing inorganic monomers around supramolecular aggregates made of amphiphilic functional molecules.[1e] Lu et al. reported the synthesis of thin films of mesoporous silica-containing rodlike aggregates of oligoethylene glycol-functionalized diacetylene surfactants.[3] The incorporated diacetylenes were polymerized into the conjugated polymers within inorganic mesochannels. Aida et al. demonstrated the polymerization of amphiphilic diacetylene and pyrrole inside silicate channels.[4] We previously reported the fabrication of organic−inorganic composites containing one-dimensional stacks of amphiphilic disklike molecules.[5] In contrast with the former approach, this approach provides the uniform incorporation of functional molecules within a highly ordered inorganic environment.

Here, we report the synthesis of an organic−inorganic composite material templated by end-functionalized nonionic triblock copolymers. Using amphiphilic block copolymers as templates for polymerizing silica species enable the preparation of highly ordered mesoporous inorganic structures.[6] Introducing functional molecules into the ends of block copolymers might enable the creation of novel organic−inorganic composites containing highly concentrated functional molecules within the mesochannels.

Strong, highly directional noncovalent interactions such as hydrogen bonding, metal−ligand interactions, donor−acceptor interactions, and host−guest interactions allow the construction of self-assembling polymer systems (supramolecular polymers) by connecting small building units with multiple association end groups.[7−10] In contrast to conventional polymers, these supramolecular polymers can dissociate into monomer units as a result of external stimuli. In this study, terpyridine (tpy) ligands were introduced into both terminates of poly(ethylene oxide)−poly(propylene oxide)−poly(ethylene oxide) (EO−PO−EO) chains. The resulting tpy-terminated EO−PO−EO can be assembled into supramolecular polymers though the formation of bis(terpyridine)−metal complexes coordinated with transition metal ions. Terpyridine ligands have been used for the bridging ligands for well-defined metallosupramolecular structures.[11] Schubert et al. have synthesized homopolymers and block copolymers from tpy-terminated oligomers or polymers through the metal−ligand interaction.[12] We report the formation of metallosupramolecular polymers within silicate channels by using tpy-terminated EO−PO−EO triblock copolymers as both structure-directing agents and monomers.

Results and Discussion

Terpyridine-terminated EO−PO−EO **1** was prepared from 4′-chloro-2,2′:6′, 2″-terpyridine and EO−PO−EO block copolymers according to a literature method (Scheme 1).[12] A reaction of 4′-chloro-2,2′:6′,2″-terpyridine with $EO_{20}-PO_{70}-EO_{20}$ (Sigma Aldrich, number-average molecular weight ca. M_n = 5800) in the presence of powdered KOH and subsequent purification by size-exclusion chromatography (BioBeads SX-1 in THF) yielded 34% of tpy-terminated $EO_{20}-PO_{70}-EO_{20}$ **1**. The tpy-terminated block copolymer **1** were characterized by

* Authors to whom correspondence should be addressed. E-mail: mkimura@shinshu-u.ac.jp (M.K.) and hshirai@shinshu-u.ac.jp (H.S.).

10.1021/ma0476644 CCC: $30.25
Published on Web 05/13/2005

Scheme 1. Schematic Representation of $EO_{20}PO_{70}EO_{20}$ Modification with Tpy-Terminated Groups and the Formation of Metallosupramolecular Polymers

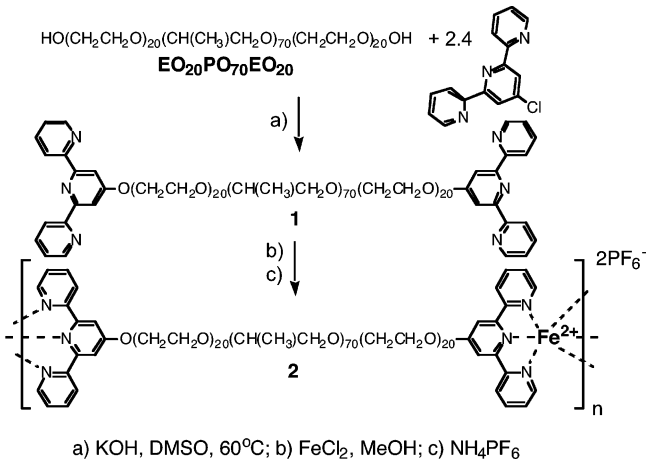

^{1}H NMR, UV−vis, gel-permeation chromatography (GPC), and MALDI-TOF-MS. The proton resonance of 3′,5′ protons for tpy appeared at 8.04 ppm, indicating the formation of an ether bond between the tpy and hydroxy end groups of the $EO_{20}-PO_{70}-EO_{20}$ chain. The GPC analysis showed that **1** had a single sharp, symmetrical elution pattern with polydispersities (M_w/M_n) of less than 1.2. The parent $EO_{20}-PO_{70}-EO_{20}$ polymers had no absorption in the UV region because of the lack of aromatic groups. On the other hand, the GPC profiles of **1** detected by a UV detector monitored at 270 nm agreed with that detected by a refractive index (RI) detector. This clearly showed the incorporation of tpy ligands into the block copolymers. Furthermore, the MALDI-TOF-MS spectra exhibited a shift of 463 Da for each single peak from the parent polymers. The difference in molecular weights corresponds to the masses of the two tpy ligand molecules. These analytical results suggested that the two tpy ligands reacted almost completely with both ends of the $EO_{20}-PO_{70}-EO_{20}$ chain.

To investigate the possibility of assembly with **1** and Fe^{2+}, the absorption spectra were monitored for varying concentrations of Fe^{2+} ions in degassed methanol (Figure 1). When the tpy ligands coodinate with octahedrally coordinating transition metal ions, stable bis(terpyridine)−metal complexes are formed between two tpy ligands and one metal ion. The absorption spectrum of **1** changed after the addition of Fe^{2+} ions, and a metal-to-ligand charge transfer (MLCT) band appeared at 568 nm, indicating the formation of a bis(terpyridine)−iron complex.[13] Furthermore, the absorbance at 568 nm increased with the Fe^{2+} concentration and then saturated.

The tpy-terminated $EO_{20}-PO_{70}-EO_{20}$ block copolymer **1** can be assembled into high-molecular-weight supramolecular polymers or cyclic oligomers. A coordination product **2** was prepared from a reaction between **1** and $FeCl_2$ in methanol and an exchange of the counterions by the addition of NH_4PF_6 (Scheme 1). The ^{1}H NMR spectrum of **2** showed the shifts for the 3′,5′ and 6,6′ protons relative to the spectrum of **1,** and it agreed with that of the corresponding low-molecular-weight bis(terpyridine) iron complex. The spectrum did not contain any peaks for the free tpy ligands as end groups of **1**. The intrinsic viscosity [θ] of **2** was 40 mL/g

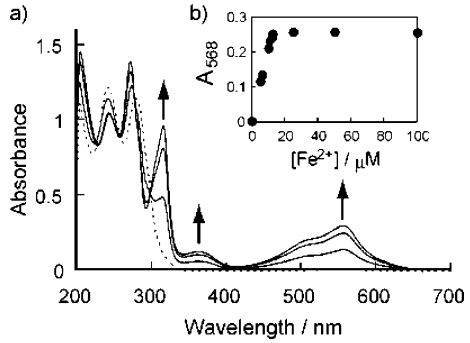

Figure 1. Effect of Fe^{2+} concentration on the absorption spectra of **1** (0.1 mg/ml) in methanol: [Fe^{2+}] = 0, 5, 10, 12.5 μM. Arrows indicate the direction of the spectral change. The inset shows the relationship between Fe^{2+} concentration and the absorbance at 568 nm.

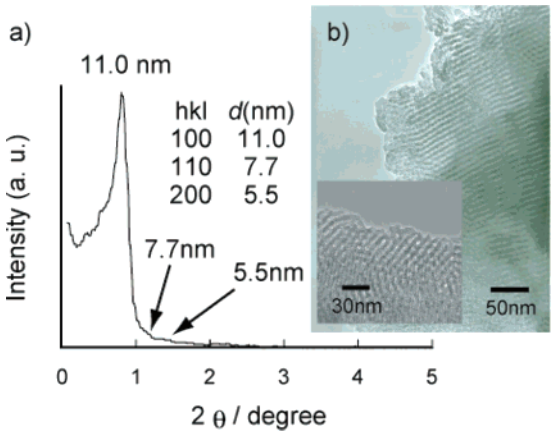

Figure 2. (a) Powder XRD pattern and (b) TEM images of the organic−inorganic composite prepared with **1**.

in methanol at 25 °C. The lack of peaks for free ligands in the ^{1}H NMR spectrum, as well as the [θ] value, implied a high degree of polymerization.[14] Furthermore, the MALDI-TOF-MS spectrum of **2** exhibited no peaks corresponding to the cyclic oligomers. These results suggested that the tpy-terminated $EO_{20}-PO_{70}-EO_{20}$ **1** could be assembled into a high-molecular-weight linear supramolecular polymer by connecting two terpyridine terminates of $EO_{20}-PO_{70}-EO_{20}$ with one Fe^{2+} ion.

Stucky and co-workers reported the preparation of well-ordered hexagonal mesoporous silica structures (SBA-15) by using amphiphilic EO−PO−EO copolymers to direct the organization of the polymerizing silica species.[6a,6b] Sol−gel polymerization of tetraethoxysilane (TEOS) in the presence of **1** was carried out under acidic conditions according to the method reported by Stucky et al.[6a] After stirring of the reaction mixture for 20 h at 35 °C, a white precipitate **3** was collected and dried at 50 °C. The product yields were above 90% on the basis of the initial amounts of silicon and the organic templates. When **3** was immersed into a methanol solution of $FeCl_2$, the color of the composites turned from white to purple, while the solution remained colorless. This suggested that the incorporated **1** was not released from the composite. Small-angle X-ray diffraction (XRD) patterns and a transmission electron microscopy (TEM) image of **3** are shown in Figure 2. The XRD patterns of **3** showed an intense peak with a d spacing of 11.0 nm and two weak peaks in the 2θ range of 1−2° with d spacing of 7.7 and 5.5 nm, which are characteristic of the (100), (110), and (200) diffractions of a hexagonal mesoscopic inorganic structure. The TEM image of **3**

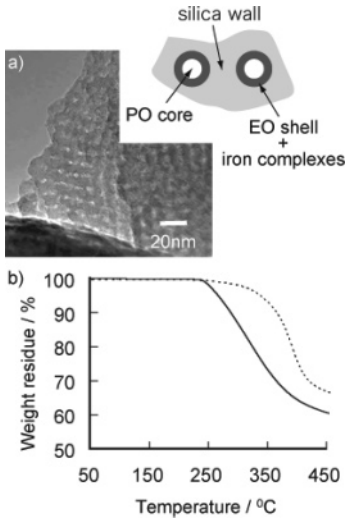

Figure 3. (a) TEM image of the organic−inorganic composite after being immersed into a solution of Fe^{2+}. The inset depicts the idealized nanostructure. (b) TGA curves of the organic−inorganic composites containing only **1** (solid line) and the composite after being immersed into a solution of Fe^{2+} (dotted line).

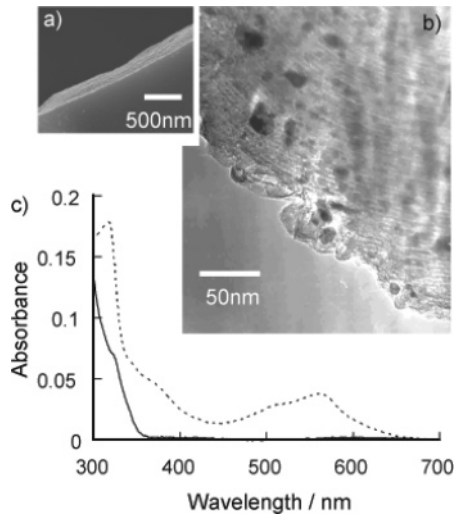

Figure 4. (a) SEM and TEM images of the spin-coated composite film prepared with **1**. (c) Absorption spectra of composite film before (solid line) and after (dotted line) being dipped in a solution of Fe^{2+}.

showed a hexagonal array of regularly sized holes with a diameter of 4.5 nm separated by ∼4.4-nm-thick silica walls. Thermogravimetric analysis (TGA) of **3** showed a weight loss of 40 wt % at 450 °C, and its FT-IR spectrum of **3** was the sum of the spectra of **1** and silica. After calcination of **3** in air at 500 °C for 6 h, the XRD pattern and TEM image showed that the hexagonal morphology had been preserved. The calcinated sample had a mean pore size of 3.6 nm, a pore volume of 0.58 cm^3/g, and a Brunauer−Emmett−Teller (BET) surface area of 641 m^2/g, as determined from N_2 adsorption−desorption experiments. These results are very similar with those for SBA-15 prepared with $EO_{20}-PO_{70}-EO_{20}$ as a template under the same conditions,[6a] indicating that tpy-terminated $EO_{20}-PO_{70}-EO_{20}$ acts as a structure-directing reagent in the creation of a hexagonal mesostructure. Therefore, we concluded that tpy-terminated $EO_{20}-PO_{70}-EO_{20}$ **1** is filled within highly ordered mesoporous silica channels.

Figure 3a shows a TEM image of **3** that had been immersed into the methanol solution of $FeCl_2$. The average diameter of the white circular regions was 3.0 nm, and the average thickness of the dark wall regions was ∼7.0 nm. The diameters of the white circles were reduced from 4.5 to 3.0 nm by the addition of $FeCl_2$.[15] The white circular regions were predominately the hydrophobic PO cylinder cores, while the dark walls consisted of silica and EO shells containing the iron complexes.[16] Energy-dispersive X-ray analysis (EDXA) also indicated the presence of Fe and Cl within the composites. While the weight of **3** was gradually decreased from 250 °C in the TGA analysis, the weight loss for the composites after immersion into the $FeCl_2$ solution started from 300 °C (Figure 3b). These results showed that the metallosupramolecular polymers were filled within the mesochannels and the tpy segments located in the hydrophilic EO shells formed bis(terpyridine)−iron complexes. In addition, the formation of the iron complexes contributed to the thermal stability of the organic−inorganic composites.

Mesostructured silica composite films containing **1** were prepared from a homogeneous ethanol/water solution of silicic acid and **1** on a quartz substrate by an evaporative spin-coating procedure.[17] The spin-coating of the aqueous solution on the substrate produced homogeneous, transparent films, which were dried in air for 24 h at room temperature and then for an additional 3 h at 120 °C to promote the formation of silica networks. Scanning electron microscopy (SEM) images indicated that the spin-coated films containing **1** were featureless at the micrometer-length scale and had thicknesses of 700−800 nm, as shown in Figure 4a.

The XRD pattern of a silica film showed a sharp peak, and the *d* spacing of this peak almost agreed with that of the powdered sample of **3**. A TEM image of the film shows well-defined strips (Figure 4b) and a hexagonal array of pores 4.8 nm in diameter. These results indicated the formation of highly ordered mesoporous silica channels within the transparent cast film by the evaporative spin-coating procedure. When a spin-coated film was dipped for 1 min in a 0.2 M methanol solution of $FeCl_2$ and washed with methanol several times, the film was stained purple as a result of the formation of iron complexes with included tpy terminates. Figure 4c shows the change in the absorption spectrum of a composite film containing **1** after immersion in the Fe^{2+} solution. The MLCT band at 568 nm appeared with the addition of $FeCl_2$, similar to the case in solution, indicating the formation of bis(terpyridine)−iron complexes within the composite film. Moreover, the MLCT band disappeared when the film was immersed in an ammonia solution for 1 min. The iron complexes within the mesochannels were decomposed by a ligand substitution reaction between the tpy ligands and the ammonia.[18] The surface hardness of composite film was evaluated by the pencil hardness test. The hardness increased from 4B to H (pencil hardness) because of the formation of metallosupramolecular polymers within the mesochannels.

In conclusion, we demonstrated the creation of organic−inorganic composites containing a tpy-terminated amphiphilic block copolymer $EO_{20}-PO_{70}-EO_{20}$. The tpy-terminated $EO_{20}-PO_{70}-EO_{20}$ could act as a template for forming a hexagonal array of mesochannels (Figure 5). The functionalized block copolymers were included within the mesochannels and the incorporated copolymers were not released from the composites by

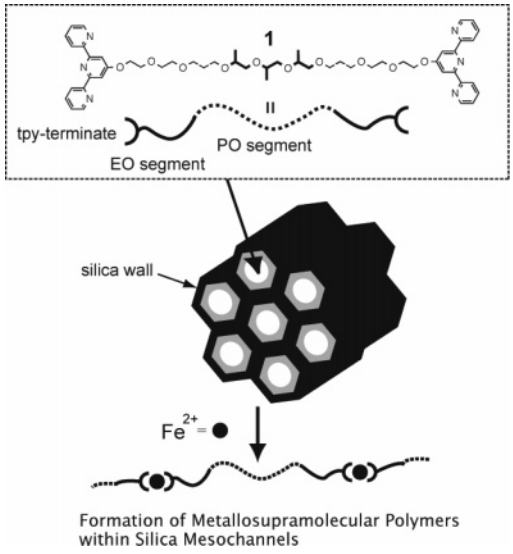

Figure 5. Schematic representation of the template synthesis of the organic−inorganic composites prepared with **1** and formation of metallosupramolecular polymers within the mesochannels.

washing with solvents or by heating. The formation of metallosupramolecular polymers within the mesochannels improved thermal stability and film hardness. Furthermore, this composite film containing tpy-terminated $EO_{20}-PO_{70}-EO_{20}$ could be used to sense metal ions through monitoring of the absorption spectrum changes. The tpy ligands can coordinate with many transition metals, and the absorption spectrum or color of the film was changed by the formation of metal complexes within the mesochannels. The spectrum and color were then recovered by decomposing the metal complexes. Modification of the end groups of amphiphilic block copolymers with functional units should enable the construction of highly integrated and stable organic−inorganic composites. The incorporated functional units will display their functionality within the mesochannels. This approach could be applied to the development of nanostructured optoelectronic materials and highly sensitive chemosensors.

Experimental Section

General. NMR spectra were recorded on a Bruker AVANCE 400 FT-NMR spectrometer operating at 399.65 MHz for ^{1}H in $CDCl_3$ solution. Chemical shifts were reported relative to internal TMS. IR spectra were obtained on a JASCO FS-420 spectrometer as KBr pellets. UV−vis was measured on a JASCO V-570. MALDI-TOF-MS spectra were obtained on a PerSeptive Biosystems Voyager DE-Pro spectrometer with dithranol as matrix. GPC analyses were carried out with a JASCO HPLC system (pump 1580, UV detector 1575, and refractive index detector 930) and a Showa Denko GPC KF-804L column (8.0 mm × 300 mm × 2 mm, polystyrene standard M = 900−400 000 g/mol) in THF as an eluent at 35 °C (1.0 mL/min).

Field-emission (FE) scanning electron microscopy (SEM) image was obtained on a Hitachi S-4500S microscope at an accelerating voltage of 15 kV. For the FE−SEM measurement, Pt−Pd alloy was sputtered (~10 nm in thickness) onto the cross-section of the spin-coated film. Transmission electron microscopy (TEM) images were recorded on a JEOL JEM-2010 electron microscope with an accelerating voltage of 200 kV. The samples for TEM were prepared by dispersing a powder or a scraped spin-coated film of products through a slurry in methanol onto a carbon film on a copper grid. Small-angle X-ray powder diffraction (XRD) patterns were taken on a MAC Science M06XCE diffractometer using Cu Kα radiation. The nitrogen adsorption and desorption isotherms at 77K was measured using a Micromeritics TriStar 3000 system.

Materials. All chemicals were purchased from commercial suppliers and used without purification. All solvents were distilled before each procedure.

1: To a suspension of powdered KOH (0.53 g, 9.45 mmol) in dry DMSO, $EO_{20}PO_{70}EO_{20}$ (Sigma Aldrich, number-average molecular weight ca. M_n = 5800 g/mol) (2.6 g) was added. After stirring at room temperature for 10 min, 4′-chloro-2,2′:6′,2″-terpyridine (0.3 g, 1.12 mmol) was added. The mixture was stirred for 120 h at 60 °C. The solvent was removed in vacuo, and the residue was purified by SEC (BioBeads SX-1 in THF). Yield 0.98 g. ^{1}H NMR ($CDCl_3$): d = 1.12−1.15 (−CH_3), 3.40 (−CH−), 3.53−3.64 (−CH_2−), 7.32 (dd, J = 7.32 Hz, H$^{5,5''}$, 4H), 7.84 (m, H$^{4,4''}$, 4H), 8.04 (s, H$^{3'/5'}$, 4H), 8.61 (d, J = 8.08 Hz, H$^{3,3''}$, 4H), 8.68 (d, J = 4.80 Hz, H$^{6,6'}$, 4H). MALDI-TOF-MS: M_w, 7524 g/mol; PDI, 1.08. GPC (THF, polystyrene standard): M_w, 7500 g/mol; PDI, 1.09.

2: To a solution of **1** (60 mg) in 5 mL methanol, a solution of iron(II) chloride dihydrate (1.34 mg, 10.6 mmol) in 2 mL methanol was added, and the mixture was stirred for 4 h at room temperature. The solution was then treated with a solution of ammonium hexafluorophosphate (13.8 mg, 84.7 mmol). The solvent was removed in vacuo, and the residue was purified by SEC. Yield: 58 mg. ^{1}H NMR (CD_3OD): d = 1.06 (−CH_3), 3.38 (−CH−), 3.55−3.65 (−CH_2−), 7.13 (m, 4H), 7.20 (m, 4H), 7.88 (m, 4H), 8.60 (d, J = 7.32 Hz, 4H), 8.70 (s, 4H). MALDI-TOF-MS: M_w: 7607 g/mol.

Preparation of Powdered Organic−Inorganic Composites. 1: (50 mg) was dissolved in 0.375 mL water and 1.5 mL 2 M HCl solution with stirring. Then 0.114 mL of TEOS was added to the homogeneous solution with stirring at 35 °C for 20 h. The solid product was collected, washed with water, and dried at 50 °C.

Preparation of Composite Film. A mixture of TEOS (0.28 mL, 1.25 mmol), ethanol (0.27 mL, 4.63 mmol), and 2 N HCl solution (0.12 mL, 0.24 mmol) was reacted for 1 h at 60 °C. This solution (0.25 mL) was added to ethanol solution of **1** (33.0 mg) with stirring, and the mixture was allowed to stand for 3 h at room temperature. The resulting viscous solution was spin-coated onto a quartz substrate (rotation speed: 3000 rpm) and dried in air for 24 h at room temperature and then for an additional 3 h at 120 °C.

Acknowledgment. This work was partially supported by a Grant-in-Aid for the 21st Century COE Program and Scientific Research (No. 15750154) from the Ministry of Education, Culture, Sports, Science, and Technology, Japan.

Supporting Information Available: Nitrogen adsorption−desorption isotherm and pore size distribution curve for the calcinated sample, and XRD pattern of mesostructured silica film. This material is available free of charge via the Internet at http://pubs.acs.org.

References and Notes

(1) (a) Ying, J. Y.; Mehnert, C. P.; Wong, M. S. *Angew. Chem., Int. Ed.* **1999**, *38*, 56 and references therein. (b) Asefa, T.; Yoshina-Ishii, C.; MacLachlan, M. J.; Ozin, G. A. *J. Mater. Chem.* **2000**, *10*, 1751. (c) Tajima, K.; Aida, T. *Chem. Commun.* **2000**, 2399. (d) Wirnsberger, G.; Stucky, G. D. *ChemPhysChem.* **2000**, *1*, 89. (e) Stein, A. *Adv. Mater.* **2003**, *15*, 763. (e) Kageyama, K.; Tamazawa, J.; Aida, T. *Science* **1999**, *285*, 2113.

(2) For example: (a) Wu, C.-G.; Bein, T. *Science* **1994**, *264*, 1757. (b) Nguyen, T.-Q.; Wu, J.; Doan, V.; Schwartz, B. J.; Tolbert, S. H. *Science* **2000**, *288*, 652.

(3) Lu, Y.; Yang, Y.; Sellinger, A.; Lu, M.; Hung, J.; Fan, H.; Haddad, R.; Lopez, G.; Burns, A. R.; Sasaki, D. Y.; Shelnutt, J.; Brinker, C. J. *Nature* **2001**, *410*, 913.

(4) (a) Aida, T.; Tajima, K. *Angew. Chem., Int. Ed.* **2001**, *40*, 3803. (b) Okabe, A.; Fukushima, T.; Ariga, K.; Aida, T. *Angew.*

Chem., Int. Ed. **2002**, *41*, 3414. (c) Ikegame, M.; Tajima, K.; Aida, T. *Angew. Chem., Int. Ed.* **2003**, *115*, 2204.
(5) (a) Kimura, M.; Wada, K.; Ohta, K.; Hanabusa, K.; Shirai, H.; Kobayashi, N. *J. Am. Chem. Soc.* **2001**, *123*, 2438. (b) Kimura, M.; Wada, K.; Iwashima, Y.; Ohta, K.; Hanabusa, K.; Shirai, H.; Kobayashi, N. *Chem. Commun.* **2003**, 2504.
(6) (a) Zhao, D.; Feng, J.; Huo, Q.; Melosh, N.; Fredrickson, G. H.; Chmelka, B. F.; Stucky, G. D. *Science* **1998**, *279*, 548. (b) Zhao, D.; Huo, Q.; Feng, J.; Chmelka, B. F.; Stucky, G. D. *J. Am. Chem. Soc.* **1998**, *120*, 6024. (c) Finnefrock, A. C.; Ulrich, R.; Du Chesne, A.; Honeker, C. C.; Schumacher, K.; Unger, K. K.; Gruner, S. M.; Wiesner, U. *Angew. Chem., Int. Ed.* **2001**, *40*, 1208.
(7) Lehn, J.-M. *Supramolecular Chemistry: Concepts and Perspectives*; VCH: Weinheim, **1995**.
(8) (a) Sijbesma, R. P.; Beijer, F. H.; Brunsveld, L.; Folmer, B. J. B.; Ky Hischberg, J. H. K.; Lange, R. F. M.; Lowe, J. K. L.; Meijer, E. W. *Science* **1997**, *278*, 1601. (b) Brunsveld, L.; Folmer, B. J. B.; Meijer, E. W.; Sijbesma, R. P. *Chem. Rev.* **2001**, *101*, 4071 and references therein.
(9) (a) Baxter, P. N. W.; Lehn, J.-M.; Fischer, J.; Youinou, M.-T. *Angew. Chem., Int. Ed. Engl.* **1994**, *33*, 2284. (b) Michelson, U.; Hunter, C. A. *Angew. Chem., Int. Ed.* **2000**, *39*, 764. (c) Krämer, R.; Lehn, J.-M.; Marquis-Rigault, A. *Proc. Natl. Acad. Sci. U.S.A.* **1993**, *90*, 5394.
(10) (a) Yamaguchi, N.; Gibson, H. W. *Angew. Chem., Int. Ed.* **1999**, *38*, 143. (b) Harada, A.; Li. J.; Kamachi, M. *Nature* **1992**, *356*, 325. (c) Hoshino, T.; Kawaguchi, A.; Harada, A. *J. Am. Chem. Soc.* **2000**, *122*, 9876.
(11) (a) Newkome, G. R.; He, E.; Moorefield, C. N. *Chem. Rev.* **1999**, *99*, 1689 and references therein. (b) Chembron, J.-C.; Dietrich-Buchecker, C.; Sauvage, J.-P. In *Comprehensive Supramolecular Chemistry*; Atwood, J. L., Davis, J. E. D., Macnicol, D. D., Vögtle, F., Eds.; Pergamon: Elmsford, NY, 1996; Vol. 9, p 43. (c) Schütte, M.; Kurth, D. G.; Linford, M. R.; Cölfen, H.; Möhwald, M. *Angew. Chem., Int. Ed. Engl.* **1998**, *37*, 2891. (d) Lehmann, P.; Kurth, D. G.; Brezesinski, G.; Symietz, C. *Chem.—Eur. J.* **2001**, *7*, 1646.
(12) (a) Lohmeijer, B. G. G.; Schubert, U. S. *Angew. Chem., Int. Ed.* **2002**, *41*, 3825. (b) Heller, M.; Schubert, U. S. *Macromol. Rapid Commun.* **2001**, *22*, 1358. (c) Schmatloch, S.; Fernández González, M.; Schubert, U. S. *Macromol. Rapid. Commun.* **2002**, *23*, 957. (d) Schubert, U. S.; Hien, O.; Exchbaumer, C. *Macromol. Rapid. Commun.* **2000**, *21*, 1156. (e) Meier, M. A. R.; Lohmeijer, B. G. G.; Schubert, U. S. *Macromol. Rapid. Commun.* **2003**, *24*, 852. (f) Gohy, J.-F.; Lohmeijer, B. G. G.; Schubert, U. S. *Chem.—Eur. J.* **2003**, *9*, 3472. (g) Hofmeier, H.; El-Ghayoury, A.; Schenning, A. P. H. J.; Schubert, U. S. *Chem. Commun.* **2004**, 318. (h) Gohy, J.-F.; Lohmeijer, B. G. G.; Alexeev, A.; Wang, X.-S.; Manners, I.; Winnik, M. A.; Schubert, U. S. *Chem.—Eur. J.* **2004**, *10*, 4315. (i) Andres, P. R.; Schubert, U. S. *Adv. Mater.* **2004**, *16*, 1043.
(13) (a) Potts, K. T.; Usifer, D. A.; Guadalupe, A.; Abruna, H. D. *J. Am. Chem. Soc.* **1987**, *109*, 3. (b) Hanabusa, K.; Nakamura, A.; Koyama, T.; Shirai, H. *Macromol. Chem.* **1992**, *193*, 1309. (c) Constable, E. C.; Heirtzler, F.; Neuburger, M.; Zehnder, M. *J. Am. Chem. Soc.* **1997**, *119*, 5606. (d) Kimura, M.; Sano, M.; Muto, T.; Hanabusa, K.; Shirai, H. *Macromolecules* **1999**, *32*, 7951.
(14) (a) Knapp, R.; Schott, A.; Rehahn, M. *Macromolecules* **1996**, *29*, 478. (b) Kelch, S.; Rehahn, M. *Macromolecules* **1997**, *30*, 6185.
(15) The XRD pattern of **3** after immersion into the methanol solution of $FeCl_2$ solution showed a sharp peak at 10.8 nm.
(16) Hillmyer, M. A.; Lipic, P. M.; Hajduk, D. A.; Almdal, K.; Bates, F. S. *J. Am. Chem. Soc.* **1997**, *119*, 2749.
(17) (a) Ogawa, M. *Chem. Commun.* **1996**, 1149. (b) Besson, S.; Ricolleau, C.; Gacoin, T.; Jacquiod, C.; Boilot, J. *Microporous and Mesoporous Mater.* **2003**, *60*, 43.
(18) Kimura, M.; Horai, T.; Hanabusa, K.; Shirai, H. *Adv. Mater.* **1998**, *10*, 459.

MA0476644